

# Supporting Information

Dammermann et al. 10.1073/pnas.0809997106

## SI Methods

**Materials.** Fura-2/AM was purchased from Calbiochem. DMSO and probenecide were supplied by Sigma.

**Chemistry.**  $^1\text{H}$  NMR,  $^{13}\text{C}$  NMR, and  $^{31}\text{P}$  NMR spectra were collected in DMSO or  $\text{D}_2\text{O}$ , either on a JEOL Delta at 270 MHz ( $^1\text{H}$ ) or 68 MHz ( $^{13}\text{C}$ ) or on a Varian Mercury-vx machine at 400 MHz ( $^1\text{H}$ ) or 100 MHz ( $^{13}\text{C}$ ). Abbreviations for splitting patterns are described below: s (singlet); d (doublet); t (triplet); and m (multiplet); etc. Low-resolution FAB and accurate mass spectra were recorded on a Micromass Autospec instrument on samples in a *m*-nitrobenzyl alcohol matrix at the Mass Spectrometry Centre, University of Bath. HPLC analysis was carried out on a Waters 2695 Alliance module equipped with a photodiode array detector and a XTerra MSC<sub>18</sub> 3.5  $\mu\text{m}$  (4.6  $\times$  150 mm) column. All samples were eluted with a gradient of MeCN against  $\text{H}_2\text{O}$  (component as specified) at 1 mL/min and monitored at 254 nm.

**Synthesis of 3-Carboxy-1-octylcarbamoylmethyl-pyridinium Bromide (BZ194).** To a stirred solution of 2-bromoacetyl bromide (12 mmol) in ether (10 mL) in an ice-salt bath was added dropwise a solution of *n*-octylamine (24 mmol) in ether (10 mL) over 30 min. The resulting reaction mixture was stirred in ice-salt bath for 15–30 min and then quenched by addition of cold water (20 mL). The organic layer was separated and washed successively with hydrochloric acid solution (1 M, 2  $\times$  20 mL), NaOH solution (1 M, 2  $\times$  20 mL) and brine (2  $\times$  20 mL). The solvent was removed and the residual 2-bromoacetyl amide was dried in vacuo. The crude product was purified by column chromatography, eluted with DCM-hexane 10:1 and then DCM to give the 2-bromo-*N*-octylacetamide as a yellow oil (71%);  $^1\text{H}$  NMR ( $\text{CDCl}_3$ , 400 MHz)  $\delta$  6.52 (brs, 1H, NH), 3.92 (s, 2H,  $\text{CH}_2\text{CO}$ ), 3.30 (s, 2H,  $\text{CH}_2\text{N}$ ), 1.56 (m, 2H,  $\text{CH}_2$ ), 1.31 (m, 10H, 5  $\times$   $\text{CH}_2$ ), and 0.91 (t,  $J = 6.5$  Hz, 3H,  $\text{CH}_3$ );  $^{13}\text{C}$  NMR ( $\text{CDCl}_3$ , 100 MHz)  $\delta$  165.2 (C), 40.3, 31.8, 29.5, 29.3, 29.21, 29.18, 26.8, 22.7 (all  $\text{CH}_2$ ), and 14.1 ( $\text{CH}_3$ ); HRMS Calcd. for  $[\text{M}+\text{H}]^+$   $\text{C}_{10}\text{H}_{21}^{79}\text{BrNO}^+$  (FAB $^+$ ) 250.0807; found: 250.0801; Calcd. for  $[\text{M}+\text{H}]^+$   $\text{C}_{10}\text{H}_{21}^{81}\text{BrNO}^+$  252.0786; found: 252.0787. Nicotinic acid (1.62 mmol) and 2-bromo-*N*-octylacetamide (1.62 mmol) were dissolved in dry DMF (4 mL) and the reaction solution was heated at 60–70  $^\circ\text{C}$  overnight. DMF was evaporated in vacuo and the resulting residue was dissolved in small amount of MeOH. The product was precipitated as a white solid by dropwise addition of ether. Purification using flash column chromatography, eluting with a gradient of 0–10% MeOH against DCM gave the title compound as a white solid (507 mg, 84%), which was checked for homogeneity by HPLC. The title compound was further purified by crystallization in MeOH/acetone giving BZ194 as a needle-like crystalline solid; mp: 195–197  $^\circ\text{C}$ ;  $^1\text{H}$  NMR (DMSO, 270 MHz)  $\delta$  9.45 (s, 1H,  $\text{H}_\text{N-2}$ ), 9.07 (s,  $J_{6,5} = 5.9$  Hz, 1H,  $\text{H}_\text{N-6}$ ), 8.94 (s,  $J_{4,5} = 8.2$  Hz, 1H,  $\text{H}_\text{N-4}$ ), 8.51 (m, 1H, NH), 8.22 (dd,  $J_{5,4} = 8.2$  Hz and  $J_{5,6} = 5.9$  Hz, 1H, H-5), 5.45 (s, 2H,  $\text{CH}_2\text{CO}$ ), 3.03 (m, 2H,  $\text{CH}_2$ ), 1.39–1.18 (m, 12H, 6  $\times$   $\text{CH}_2$ ) and 0.78 (m, 3H,  $\text{CH}_3$ );  $^{13}\text{C}$  NMR (DMSO, 100 MHz)  $\delta$  164.4, 163.5, 130.9 (all C), 149.7, 147.9, 146.4, 128.1 (all CH), 62.1, 31.7, 29.3, 29.2, 29.1, 26.8, 22.6 (all  $\text{CH}_2$ ), and 14.5 ( $\text{CH}_3$ ); HRMS (FAB $^+$ ) Calcd. for  $[\text{M}]^+$   $\text{C}_{16}\text{H}_{25}\text{N}_2\text{O}_3^+$  293.1865 found 293.1870;  $t\text{R} = 7.3$  min; solvent: 20–95% MeCN against  $\text{H}_2\text{O}$  over 25 min.

**Antigens.** Antigen-specific T cell clones were specific for guinea pig myelin basic protein (MBP), ovalbumin (OVA), or S100 $\beta$ .

OVA and S100 $\beta$  were obtained from Sigma. MBP was purified from guinea pig brains as reported (1). A peptide comprising human myelin basic protein amino acids 139 to 153 (hMBP139–153) (KGFKGVDAQGTLISKI) was synthesized by Fmoc chemistry and purified by preparative C8 reverse-phase HPLC. Tetanus toxoid (TT) containing no preservatives was obtained from Behringwerke.

**Generation and Culturing of T Cells.** MBP-, OVA-, and S100 $\beta$ -specific  $\text{CD4}^+$  T cells ( $\text{T}_{\text{MBP}}$ ,  $\text{T}_{\text{OVA}}$ , and  $\text{T}_{\text{S100}\beta}$ ) retrovirally engineered to express the marker gene EGFP have been generated and tested for their phenotype, cytokine profile, and antigen specificity as reported (2, 3). Briefly, following immunization with specific antigen, cells from the draining lymph nodes were cultured ( $2 \times 10^7$ /plate) together with retrovirus producing GP+E 86 packaging cells. Moloney leukemia virus derivative pLXSN in which the EGFP gene cDNA (Invitrogen) had been integrated (pLGFPSN) was used as retroviral vector. Packaging cell lines producing GFP-carrying retrovirus were established as described (3). T lymphocyte blasts were expanded in IL-2 containing growth medium after 3 days coculture. Selection with G418 and amplification of the T cells was performed as reported (4).

Human MBP139–153-specific  $\text{CD4}^+$  T cell lines were established by the standard split-well method (5). Briefly, PBMCs were seeded in 200  $\mu\text{L}$  RPMI medium (Invitrogen/Gibco) containing 7.5% pooled human AB serum (Sigma), in the presence of 28  $\mu\text{M}$  hMBP139–153. Every 3 to 4 days, 100  $\mu\text{L}$  medium was substituted by fresh medium containing 5 U recombinant human IL-2 (Roche). After 2 weeks, the cells were split into 2 wells.  $10^5$  irradiated autologous PBMCs were added to both wells, but hMBP139–153 was added to one of the wells only. The cultures were judged microscopically for hMBP139–153-specific proliferation. After 4 rounds of restimulation of individual lines, 9 lines were pooled for further experiments.

**Analysis of  $[\text{Ca}^{2+}]_i$ .**  $[\text{Ca}^{2+}]_i$  was determined either in Fura-2-loaded human Jurkat T cells or in rat  $\text{T}_{\text{MBP}}$  cells which had been preincubated with BZ194 or DMSO at the indicated concentrations for at least 8 h as described previously (6). For ratiometric  $\text{Ca}^{2+}$  imaging thin glass coverslips (0.1 mm) were coated with BSA (5 mg/mL) and polyL-lysine (0.1 mg/mL). Silicon grease was used to seal small chambers consisting of a rubber O-ring on the glass coverslips. Sixty  $\mu\text{L}$  buffer A (140 mM NaCl, 5 mM KCl, 1 mM  $\text{MgSO}_4$ , 1 mM  $\text{CaCl}_2$ , 1 mM  $\text{NaH}_2\text{PO}_4$ , 5.5 mM glucose, and 20 mM Hepes, pH 7.4) and a 40- $\mu\text{L}$  cell suspension ( $2 \times 10^6$  cells/mL) dissolved in the same buffer were added into the small chamber. The coverslip with cells slightly attached to the BSA/polyL-lysine coating was mounted on the stage of a fluorescence microscope (Leica DM IRE2). Alternatively, rat F10 astrocytes with up-regulated MHC II expression were cultured on  $\mu$ -slides 8 well (ibidi) on fibronectin and pulsed or not with MBP (10  $\mu\text{g}/\text{mL}$ , 2 h). Ratiometric  $\text{Ca}^{2+}$  imaging was performed as described recently (7). We used an Improvion imaging system built around the Leica microscope at 40-fold (astrocyte–T cell interaction) or 100-fold (microinjection of Jurkat T cells) magnification. Illumination at 340 and 380 nm was carried out using a monochromator system (Polychromator IV, TILL Photonics). Images were taken with a gray-scale CCD camera (type C4742–95-12ER; Hamamatsu) operated in 8-bit mode. The spatial resolution was 512  $\times$  640 pixel, the acquisition rate was approximately 1 ratio in 160 ms (microinjection experiments) or in 10 s

(T cell-astrocyte interaction experiments). Raw data images were stored on a hard disk. Confocal  $\text{Ca}^{2+}$  images were obtained by off-line no neighbor deconvolution using the volume deconvolution module of the Openlab software as described recently for 3T3 fibroblasts (8). The deconvolved images were used to construct ratio images (340/380). Finally, ratio values were converted to  $\text{Ca}^{2+}$  concentrations by external calibration. To reduce noise, ratio images were subjected to median filter ( $3 \times 3$ ) as described previously (7). Data processing was performed using Openlab software (Improvision).

**Microinjections.** We used an Eppendorf system (transjector type 5246, micromanipulator type 5171, Eppendorf) with Femtotips I as pipettes. NAADP, cADPR, and  $\text{InsP}_3$  were diluted to their final concentration in intracellular buffer (20 mM Hepes, 110 mM KCl, 2 mM  $\text{MgCl}_2$ , 5 mM  $\text{KH}_2\text{PO}_4$ , and 10 mM NaCl, pH 7.2) and filtered (0.2  $\mu\text{m}$ ) before use. In co-injection experiments BZ194 was dissolved in DMSO and mixed with various stock solutions containing NAADP, cADPR, or  $\text{InsP}_3$ . To avoid any contamination of  $\text{Ca}^{2+}$  in the solution to be injected, a small amount of Chelex resin beads was added. Injections were made using the semiautomatic mode of the system with the following instrumental settings: injection pressure, 60 hPa; compensatory pressure, 30 hPa; injection time, 0.5 s; and velocity of the pipette, 700  $\mu\text{m/s}$ . Under such conditions, the injection volume was 1–1.5% cell volume (9).

**Analysis of NFAT1 Translocation.** Resting  $T_{\text{MBP}}$  cells were treated for 16 h with BZ194 0.5 mM or DMSO, then plated on coated-glasses (100  $\mu\text{g/mL}$  rat collagen type I, BD Biosciences) and stimulated with  $\alpha\text{CD3/CD28}$  MABs in presence of 0.5 mM BZ194 or DMSO. Samples were fixed in PFA 4% 0, 30, or 60 min after stimulation. Immunohistochemical staining was performed in 1% Tryton X-100 containing PBS, using mouse monoclonal antibody against NFAT-1 (Abcam) or isotype control (Sigma-Aldrich). Cy5-labeled anti-mouse antibody (Jackson ImmunoResearch) was used as secondary antibody. DAPI was chosen for nuclear staining. Immunofluorescence analysis was carried out using a Leica confocal laser scanning microscope (Leica Inc.) using a 40 $\times$  oil objective.

**Proliferation Assays of Cultured Rat T Cells.** In addition to the methods described in the full manuscript, additional proliferation assays were carried out as follows. To exclude that BZ194 treatment interferes with the T-cell proliferation machinery,  $T_{\text{MBP}}$  cell blasts 2 days following stimulation with MBP-pulsed professional APCs were incubated with increasing amounts of BZ194 and their numbers were determined 24, 48, and 96 h later by cytofluorometry. After removal of BZ194 the T cells were then re-stimulated with MBP-pulsed APCs. [ $^3\text{H}$ ]dT incorporation was used to evaluate proliferation, after a 2-day culture.

To test antigen reactivity of BZ194-treated T cells, the cells were first stimulated with MBP-pulsed APCs in the presence of

increasing amounts of BZ194 for 48 h, or in presence of vehicle alone (DMSO, control). Thereafter, the cells were re-challenged with MBP-pulsed APCs, and their proliferation rate was evaluated 2 days later by [ $^3\text{H}$ ]dT incorporation.

For stimulation of effector  $T_{\text{MBP}}$  cells by anti-CD3/anti-CD28 antibodies and PMA/ionomycin, 96-well plates were coated for 2 h at RT with 5  $\mu\text{g/mL}$  anti-CD3 and anti-CD28 antibodies (both from Serotec) in PBS. Rat  $T_{\text{MBP}}$  were plated at the final concentration of  $10^5$ /well. When needed PMA and ionomycin were added at the final concentrations of 100 and 200 ng/mL, respectively. After a 2-day culture [ $^3\text{H}$ ]dT incorporation was measured.

**Proliferation Assays of Human T Cells.** Human MBP139–153-specific T cell lines ( $3\text{--}5 \times 10^4$  cells/well) were preincubated for 45 min with BZ194 in DMSO at final concentrations of 1.0 and 0.5 mM, or with DMSO alone. Aliquots of  $10^5$  irradiated autologous PBMCs/well were preincubated for 3 h with 28  $\mu\text{M}$  hMBP peptide (amino acids 139–153), 5  $\mu\text{g/mL}$  tetanus toxoid, or without antigen. Then T cells and PBMCs were merged and after 24 h, [ $^3\text{H}$ ]dT was added and proliferation was evaluated 16 h later.

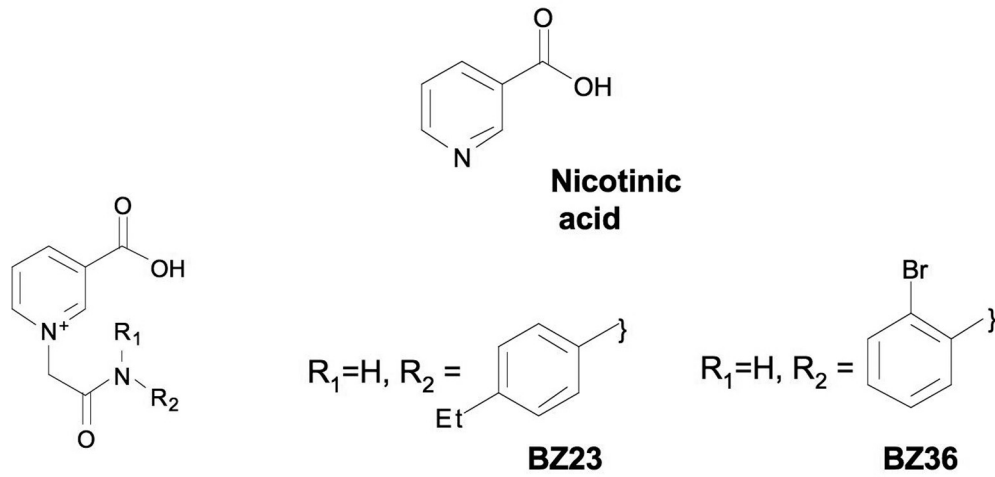
Human naive T cells were purified from PBMCs by 2-step negative selection using first a Pan T cell isolation kit and then CD45R0 MicroBeads (both MACS, Miltenyi Biotec).

**Quantitative PCR and ELISAs.** mRNA was extracted by TRIzol and reversed to cDNA using SuperScript III polymerase (Invitrogen). Taqman analysis was performed as reported using ABI Prism 5700 Sequence Detector “Taqman” (PE Applied Biosystems) (10). The expression of a housekeeping gene ( $\beta$ -actin for rat cells and GAPDH for human cells) was set into relation to the specific mRNA. Data were obtained by independent duplicate measurements. The CT value of the individual measurements did not exceed 0.5 amplification cycles. The rat primers and probes were recently described (11); the human primers and probes were kindly provided by H.-D. Volk. Cytokine protein release of rat or human T cells was measured using commercially available ELISA kits (rat IL-2 from Biosource, and human IL-2 ELISA from eBioscience).

**Immunofluorescence.** For RyR analyses rabbit anti-rat RyR1, -2, and -3 (Millipore) were used in a concentration of 1:100 in PBS/0.02% Triton X-100 containing 1% BSA. Rabbit polyclonal antibodies (Santa Cruz) served as control. As secondary antibody goat Cy3-conjugated goat anti-rabbit serum (Jackson ImmunoResearch, dilution 1:500) was used. Mouse monoclonal anti-protein disulphide isomerase (PDI) antibody (Abcam, dilution 1:100) was used to specifically mark the endoplasmic reticulum. Secondary staining was performed using Cy5-labeled goat anti-mouse antiserum. Fluorescence analyses were carried out using a Leica confocal laser scanning microscope (Leica Inc.) using a 40 $\times$  oil objective.

1. Eylar EH, Kniskern PJ, Jackson JJ (1979) Myelin basic proteins. *Methods Enzymol* 32B:323–341.
2. Kawakami N, et al. (2004) The activation status of neuroantigen-specific T cells in the target organ determines the clinical outcome of autoimmune encephalomyelitis. *J Exp Med* 199:185–197.
3. Flügel A, Willem M, Berkowicz T, Wekerle H (1999) Gene transfer into  $\text{CD4}^+$  T lymphocytes: Green fluorescent protein engineered, encephalitogenic T cells used to illuminate immune responses in the brain. *Nature Med* 5:843–847.
4. Ben-Nun A, Wekerle H, Cohen I (1981) The rapid isolation of clonable antigen-specific T lymphocyte lines capable of mediating autoimmune encephalomyelitis. *Eur J Immunol* 11:195–199.
5. Meinel E, et al. (1993) Myelin basic protein-specific T lymphocyte repertoire in multiple sclerosis: Complexity of response and dominance of nested epitopes due to recruitment of multiple T cell clones. *J Clin Invest* 92:2633–2643.
6. Guse AH, et al. (2005) A minimal structural analogue of cyclic ADP-ribose: Synthesis and calcium release activity in mammalian cells. *J Biol Chem* 280:15952–15959.
7. Kunerth S, Mayr GW, Koch-Nolte F, Guse AH (2003) Analysis of subcellular calcium signals in T-lymphocytes. *Cell Signal* 15:783–792.
8. Bruzzone S, Kunerth S, Zocchi E, De Flora A, Guse AH (2003) Spatio-temporal propagation of  $\text{Ca}^{2+}$  signals by cyclic ADP-ribose in 3T3 cells stimulated via purinergic P2Y receptors. *J Cell Biol* 163:837–845.
9. Guse AH, Berg I, da Silva CP, Potter BVL, Mayr GW (1997)  $\text{Ca}^{2+}$  entry induced by cyclic ADP-ribose in intact T-lymphocytes. *J Biol Chem* 272:8546–8550.
10. Flügel A, et al. (2001) Migratory activity and functional changes of green fluorescent effector T cells before and during experimental autoimmune encephalomyelitis. *Immunity* 14:547–560.
11. Odoardi F, et al. (2007) Instant effect of soluble antigen on effector T cells in peripheral immune organs during immunotherapy of autoimmune encephalomyelitis. *Proc Natl Acad Sci USA* 104:920–925.

A



$R_1=R_2=H$ , **CMA008**  
 $R_1=R_2=C_4H_9$  **BZ52**  
 $R_1=H, R_2=C_{10}H_{21}$  **BZ71**  
 $R_1=R_2=$  cyclohexyl (single ring) **BZ185**  
 $R_1=H, R_2=C_8H_{17}$  **BZ194**

B

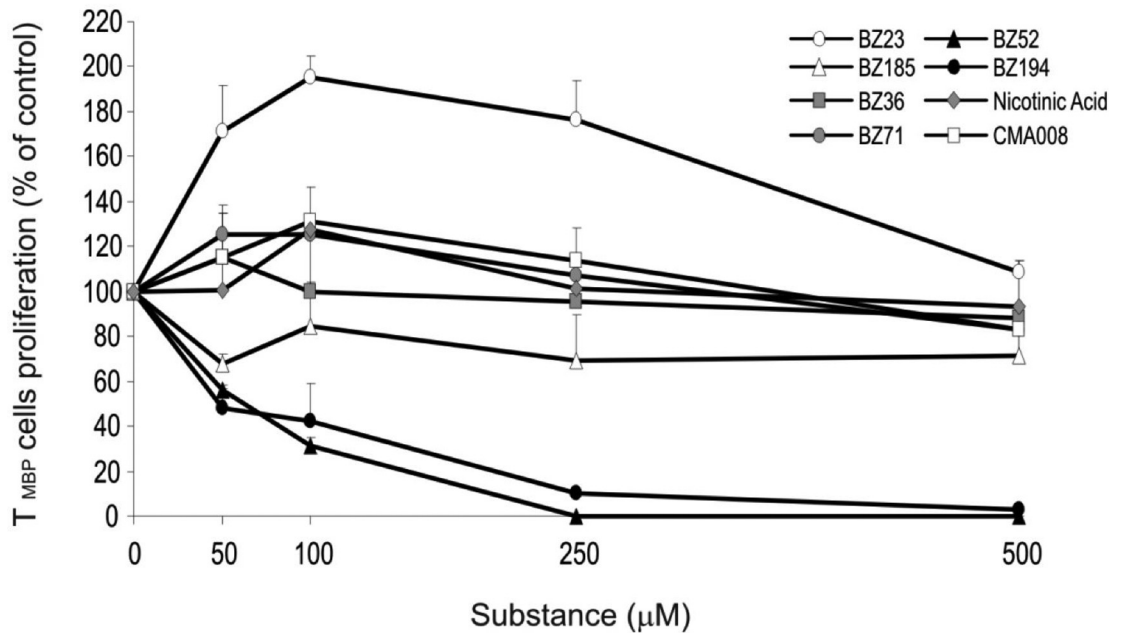


**Fig. S1.** Screening of nicotinic acid analogues as modulators for activation of effector T cells. (A) Structures of nicotinic acid and representative analogues. (B)  $T_{MBP}$  cells co-cultured with MBP-pulsed APCs were incubated with increasing amounts of the indicated BZ series ligands, CMA008, or nicotinic acid.  $T_{MBP}$  cells reactivity was determined by  $[^3H]$  dT incorporation 3 days later. Proliferation is indicated as percent of control. Mean  $\pm$  SD of triplicate measurements.

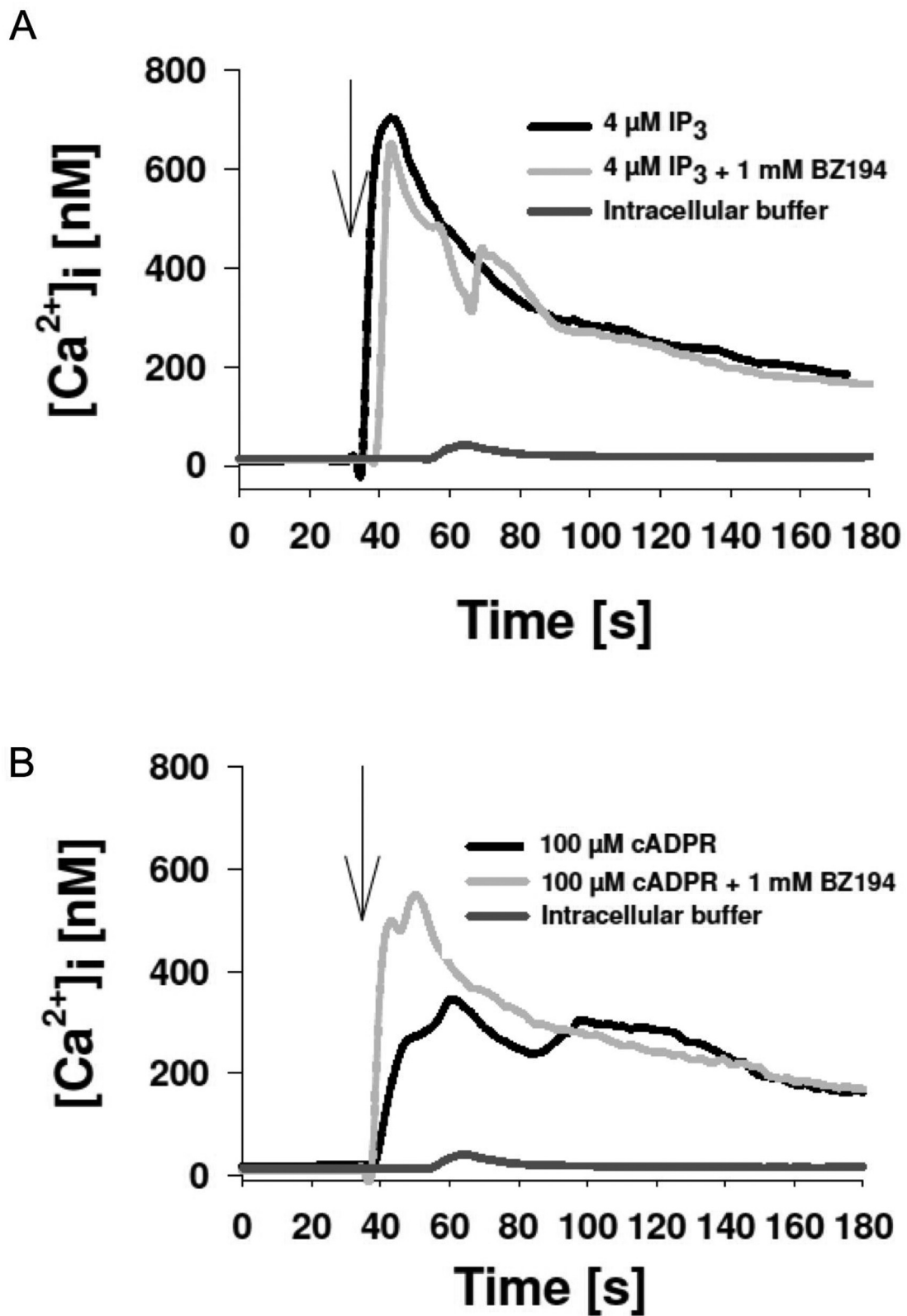


**Fig. 52.** Lack of inhibitory effect of BZ194 on Ca<sup>2+</sup> signaling induced by InsP<sub>3</sub> or cADPR. BZ194 does not directly interfere with IP<sub>3</sub>- or cADPR-mediated Ca<sup>2+</sup> release. Jurkat T cells were loaded with Fura2/AM. Thereafter, single cells were co-injected with 1 mM BZ194 and either InsP<sub>3</sub> (4 µM, *A*) or cADPR (100 µM, *B*) and Ca<sup>2+</sup> signaling was recorded. Data represent means from *n* = 5–13 individual cells.

A

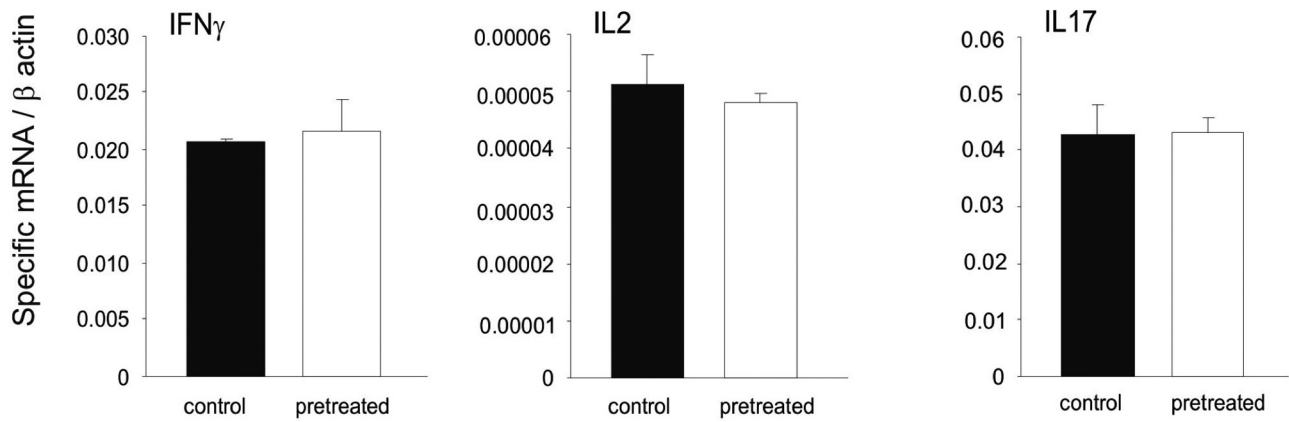


**Fig. S3.** Reconstitution of the original cytokine profile upon wash-out of BZ194. T<sub>MBP</sub> cells which had been suppressed by incubation with BZ194 (0.5 mM for 2 days; termed pretreated, white bars) or resting cultured T<sub>MBP</sub> cells (control, black bars) were specifically re-activated with MBP-pulsed APCs in the absence of BZ194. IFN $\gamma$ , IL-2, and IL-17 mRNA were analyzed using quantitative PCR 48 h later. Values are normalized to  $\beta$  actin mRNA. Shown are representative data of 2 independent experiments.

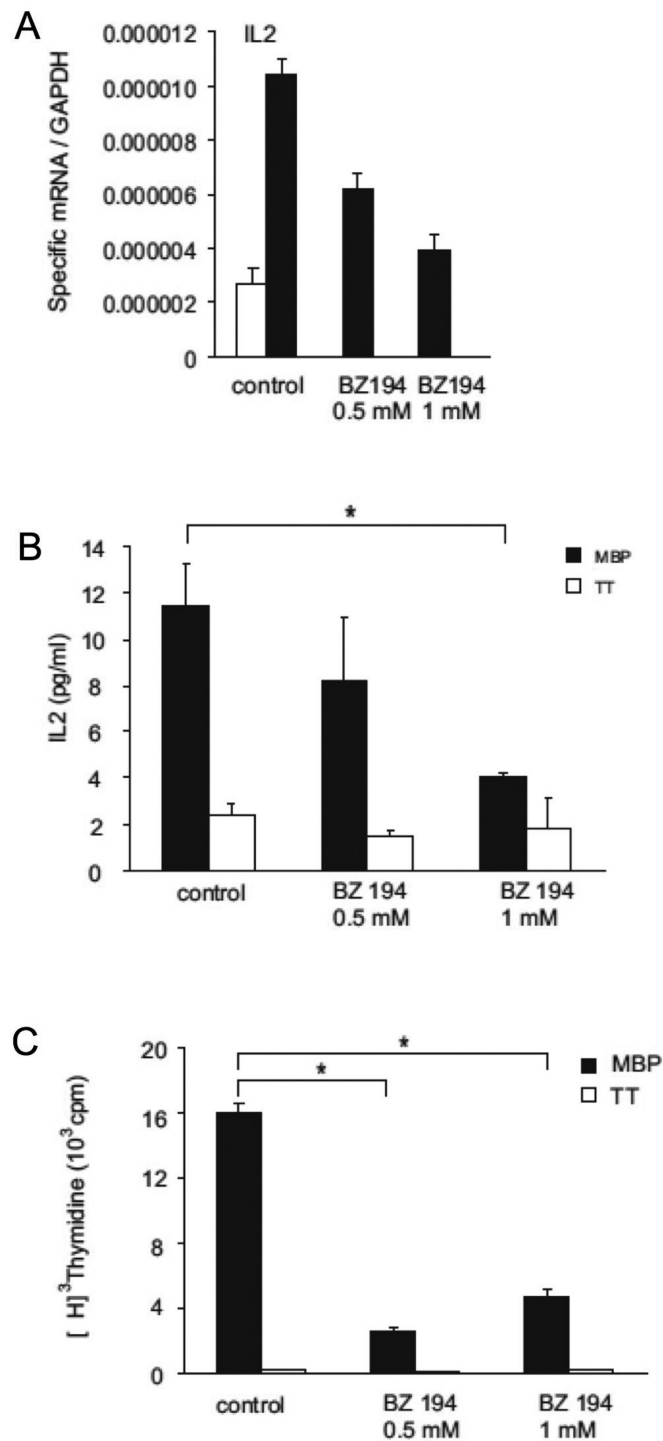


**Fig. 54.** Inhibition of human T cell activation by BZ 194. BZ194 inhibits cytokine expression and proliferation in MBP-specific CD4<sup>+</sup> T cells. (A) Quantitative PCR of human T<sub>MBP</sub> cells. mRNA was extracted 48 h after stimulation. Values are normalized to GAPDH mRNA expression. Shown are representative data of 3 independent experiments. All differences are statistically significant ( $P \leq 0.05$ ). (B) IL-2 protein release tested by ELISA. Mean  $\pm$  SD of triplicate measurements. \*,  $P \leq 0.0001$ . (C) Proliferation of human T<sub>MBP</sub> cells stimulated with MBP- (black) or tetanus toxoid (TT, white)-pulsed PBMCs in the presence of 0.5 and 1 mM BZ194 or vehicle (control). [<sup>3</sup>H] thymidine incorporation. Mean  $\pm$  SD of triplicate measurements. Representative data of 3 independent experiments. \*,  $P \leq 0.0001$ .

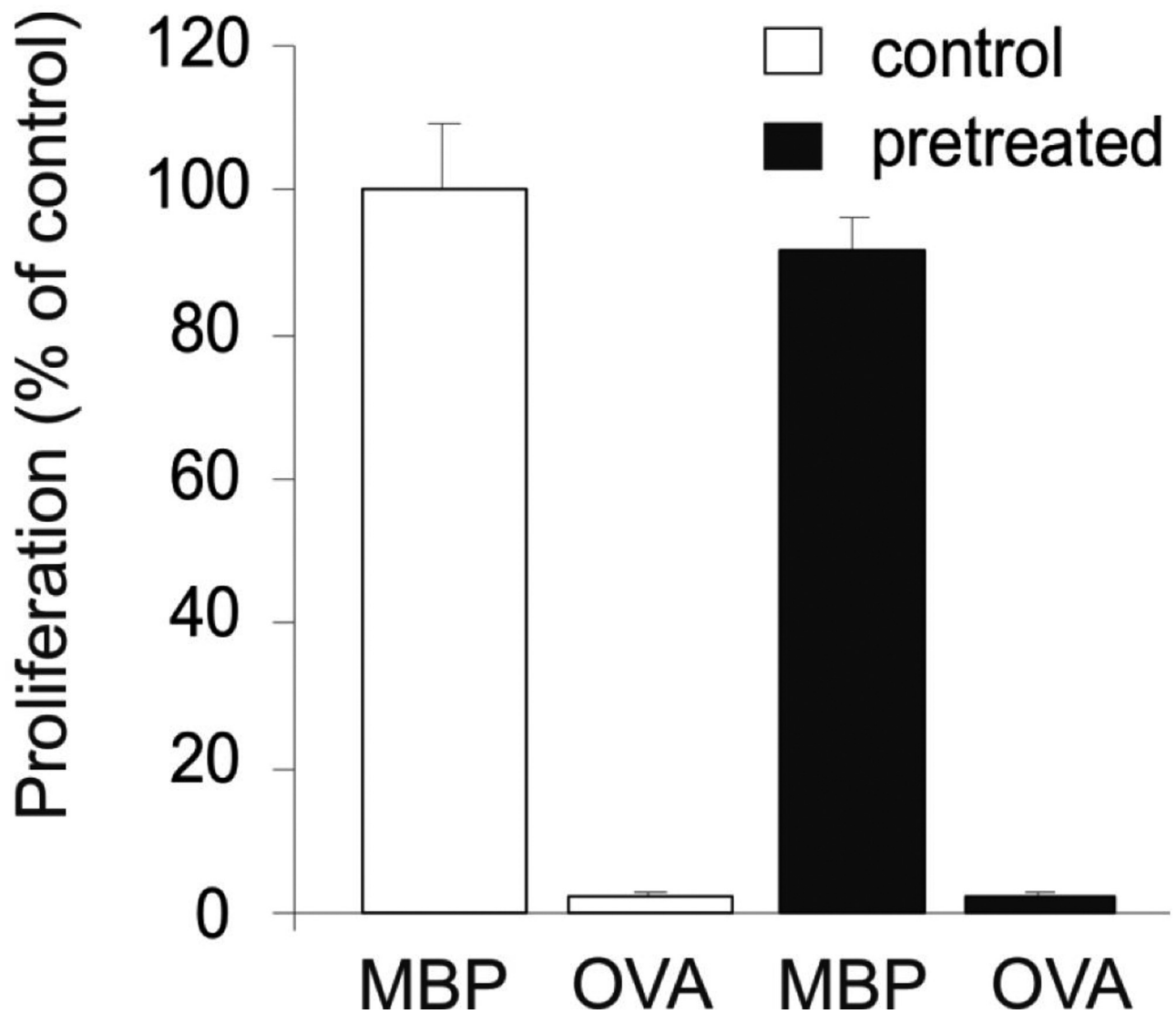


**Fig. S5.** Effect of BZ194 on T cell proliferation is reversible.  $T_{MBP}$  cells in which activation had been previously suppressed by BZ194 (0.5 mM for 2 days; termed pretreated, black bars) or resting cultured  $T_{MBP}$  cells (control, white bars) were re-exposed with MBP or OVA-pulsed APCs in the absence of BZ194. Proliferation was determined by [ $^3H$ ]dT incorporation 2 days later. Proliferation is indicated as percent of control. Mean  $\pm$  SD of triplicate measurements. Representative data of 3 independent experiments are shown.

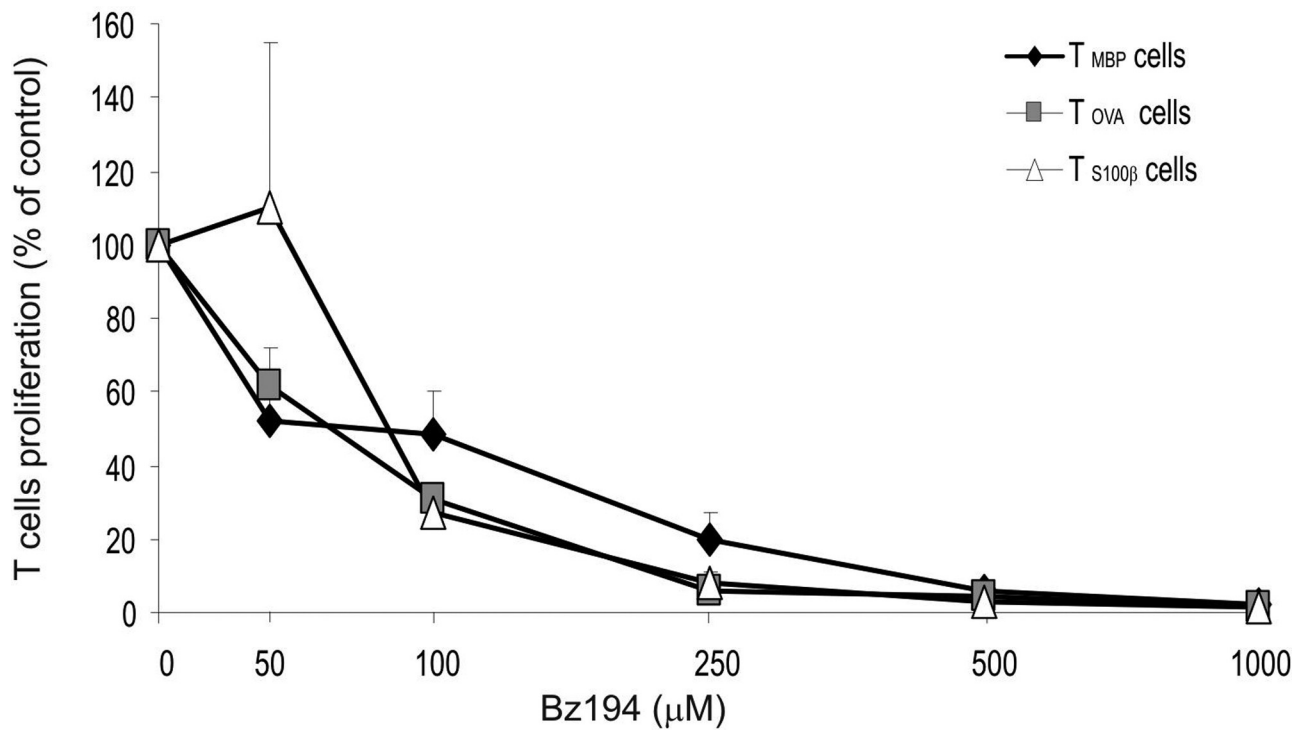


**Fig. S6.** Effect of BZ194 on antigen-specific proliferation of CD4<sup>+</sup> effector T cells. Rat T<sub>MBP</sub> (black rhombs), T<sub>OVA</sub> (gray squares), or T<sub>S100β</sub> (white triangles) cells co-cultured with MBP-, OVA- and S100β-pulsed APCs, respectively, were incubated with increasing concentrations of BZ194 and their proliferation was measured 3 days later by [<sup>3</sup>H] dT incorporation. Mean ± SD of triplicate measurements.